

The quadrilateral fully-parametrized plate elements based on the absolute nodal coordinate formulation

Marko K. Matikainen, Aki Mikkola and A. L. Schwab

Summary. The article provides a review of the quadrilateral fully-parametrized plate elements based on absolute nodal coordinate formulation that can be used in the dynamic analysis of large deformations in multibody applications. The absolute nodal coordinate formulation is a recently proposed approach to the analysis of multibody systems that can take into account nonlinearities, including large deflections and plasticity. In the absolute nodal coordinate formulation, finite elements are defined in the global coordinate system using position coordinates together with independent global gradient vectors that are, in fact, partial derivatives of the position vector with respect to the element coordinates. This leads to a constant mass matrix in two and three-dimensional applications and is a unique feature among the beam and plate elements based on the absolute nodal coordinate formulation.

Key words: nonlinear finite element method, multibody system dynamics, continuum plate elements

Introduction

Nonlinear continuum plate and shell elements have been under active research for more than four decades. Usually, these conventional continuum plate and shell elements utilize rotation parameters instead of gradient vectors. It has been previously proposed that continuum elements with fully three-dimensional stresses and strains can be degenerated to shell elements behavior so that the kinematics and constitutive assumptions of shells are acceptable; see for example [1]. The isoparametric continuum shell element introduced in [1] (known as the A-I-Z shell element) is based on the Reissner-Mindlin hypothesis. However, it is known that the A-I-Z shell element suffers from shear locking, which can be alleviated by introducing independent linear interpolations for transverse shear deformations in a four node shell element (known as the MITCH4 shell element) [2]. The original MITCH4 element is derived from the A-I-Z shell element using five nodal parameters; the only difference is that shear locking is avoided by using mixed interpolation.

A number of nonlinear finite element formulations for analyzing beam and plate type of flexible bodies in multibody dynamics have been presented. For example, in the study by Avello et al. [3], rotations and deformations of the cross-section are described by using nine parameters at a nodal location. In the study, the cross-section is forced to be rigid using constraint equations. In the dissertation by Rhim [4], the absolute motion of a spatial beam element is described using global shape functions. In the study, rotation at the nodal location is defined with two basis vectors along the cross-section as a consequence of which the beam element have nine degrees of freedom at the node. In addition, continuum based beam and plate elements in two and three-dimensional applications are proposed.

These elements are often derived from solid elements in order to account the kinematic assumptions associated to beams or shells. For these elements, any of the continuum material laws can be used, provided that the plane stress condition is valid. In order to avoid the singularity due to use of Euler rotation angles in the case of finite rotations, quaternions should be employed [5] in the formulation.

The absolute nodal coordinate formulation (ANCF) is a finite element approach in which beam and plate elements are described with an absolute position and its gradients. The formulation is designed for analysis of large deformations in multibody applications [6]. The absolute nodal coordinate formulation can be used for two or three-dimensional beams, plates and shells [7, 8, 9, 10]. Using the components of the deformation gradient instead of conventional rotational coordinates, the absolute nodal coordinate formulation leads to an exact description of inertia for the rigid body with a constant mass matrix. Therefore, the use of quaternions to avoid the singularity problem of finite rotations under three-dimensional rotations is not needed. Transverse deformations can be accounted by introducing the transverse gradient vectors. Elements based on the absolute nodal coordinate formulation can be considered as more advanced than classical beam and plate elements. In this approach, all nodal coordinates are described in an inertial frame allowing for the usage of the total Lagrangian approach, such as in the case of large rotation vector formulations and conventional solid elements. When using fully-parameterized elements, different types of locking phenomena may occur due to low order displacement interpolation in the transverse direction. In order to overcome this problem, alternative approaches are introduced to define the elastic forces, see for example [11, 12]. To clarify the absolute nodal coordinate formulation, an original fully-parameterized plate element is described in this study.

In order to define an element into the framework of the absolute nodal coordinate formulation, the element should meet several requirements. All of these requirements should also be valid in three-dimensional cases and can be expressed as follows:

- ANCF elements can be used for dynamic problems, such that the inertial forces are exactly described.
- The mass matrix should be consistent and, as a trademark of the ANCF, it should be constant. It is important to reiterate that the mass matrix is also constant for three-dimensional beam and plate elements.
- The element discretization is performed by using spatial shape functions with absolute positions and their gradients. Therefore, the Hermite base functions are usually employed in the formulation.
- ANCF elements can be considered as geometrically exact because geometrical simplifications associated to angles are not necessary to use. This leads to possibility for usage of Total Lagrangian updating formulation.

The ANCF elements can be categorized into conventional non-shear deformable elements [13] or shear deformable elements. In the formulation, shear deformation can be captured by introducing gradient coordinates in the element transverse direction. Elements that include transverse gradient vectors are often referred to as fully-parameterized elements. In this case, the elastic forces of the element can be defined by using three-dimensional elasticity or the elastic line or plane approach. In case of three-dimensional

elasticity, the strains and stresses are defined using general continuum mechanics. The elements based on three-dimensional elasticity relax some of the assumptions used in the conventional elements and they can account for the nonlinear material models in a straightforward manner. It is important to note that the use of fully-parameterized elements allows cross-sectional or fiber deformation to be described. The transverse fibers of existing plate elements based on the absolute nodal coordinate formulation remain straight, but are extensible. This implies that plate elements can be used to account for shear deformation and deformation in the thickness direction. In some elements, the transverse Poisson contraction effect can also be taken into account. It is possible to describe geometrical and material nonlinearities in the element based on three-dimensional elasticity [7, 14]. Conventional elements based on the absolute nodal coordinate formulation are discretized using global positions and gradient coordinates in the element longitudinal direction. In the elements based on this approach, strains and stresses are described on the middle line or middle plane.

Plate elements based on absolute nodal coordinate formulation

The first plate element based on the absolute nodal coordinate formulation was developed by Shabana and Christensen [15]. This plate element was based on the classical Kirchhoff-Love plate theory in which in-plane gradient vectors were used to describe bending deformation. Other Kirchhoff-Love type ANCF plates and their numerical implementations are shown in [10, 16, 17]. In order to account for the shear deformation and thickness deformation in the case of thick plates, a fully-parameterized quadrilateral plate element was developed [9]. However, this plate element suffers from slow convergence due to different locking phenomena. The plate element especially suffers from shear locking because the transverse gradient vector and in-plane gradient vectors contain different orders of polynomials. This means that in case of fully-parameterized plates, the rotation of a transverse fiber is described with linear interpolation using in-plane coordinates, and the rotation of the mid-plane is described using quadratic interpolation. The unbalance of the base functions leads to overly large shear strain, which can be alleviated by linear interpolation for transverse shear deformations [2]. The main motivation for developing the plate element in [18] was to overcome shear locking by employing linearized shear deformations. Additionally, due to the kinematic description, curvature locking (shrinking effect) can also be avoided. In this study, the original fully-parameterized plate element by Mikkola and Shabana [9] is denoted as ANCF-P48, and the improved fully-parameterized plate element [18] as ANCF-P48lsa.

Kinematics of the quadrilateral plate element

In elements based on the absolute nodal coordinate formulation, kinematics can be expressed using spatial shape functions and global coordinates. In this section, the fully-parameterized plate element by Mikkola and Shabana [9] will be shortly revisited. In Figure 1, the kinematics of the fully-parameterized plate element is shown. This four-node quadrilateral plate element consists of 48 degrees of freedom. Three degrees of freedom are for position and nine are for gradients at each node. The position of an arbitrary particle p in the fully-parameterized plate element can be defined in the inertial frame as follows:

$$\mathbf{r} = \mathbf{S}_m(\mathbf{x})\mathbf{e} = \mathbf{S}_m(\boldsymbol{\xi}(\mathbf{x}))\mathbf{e}, \quad (1)$$

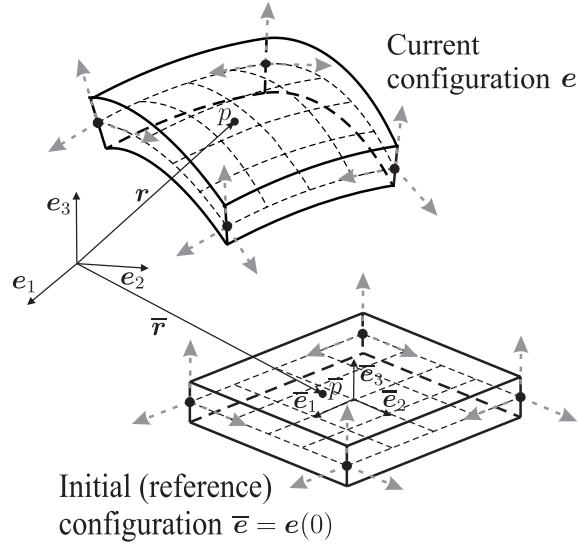


Figure 1. Description of the position of an arbitrary particle in the fully-parameterized plate element. Points \bar{p} and p refer to the same particle at different configurations after displacement. The gradient vectors at nodes are shown by dashed arrows.

where \mathbf{S}_m is a shape function matrix, $\mathbf{e} = \mathbf{e}(t)$ is the vector of nodal coordinates and vector $\mathbf{x} = x\bar{\mathbf{e}}_1 + y\bar{\mathbf{e}}_2 + z\bar{\mathbf{e}}_3$ includes physical coordinates. For the isoparametric elements, the shape functions can be expressed using physical coordinates \mathbf{x} or local coordinates $\boldsymbol{\xi}$ in the range $-1 \dots +1$. The kinematics of the element in the reference configuration at time $t = 0$ can be described as $\bar{\mathbf{r}} = \mathbf{S}_m(\mathbf{x})\bar{\mathbf{e}}$, where $\bar{\mathbf{e}} = \mathbf{e}(0)$. The vector \mathbf{e} contains both translational and rotational coordinates of the element, and it can be written at node i of the three-dimensional fully-parameterized element as follows:

$$\mathbf{e}^{(i)} = \begin{bmatrix} \mathbf{r}^{(i)T} & \mathbf{r}_{,x}^{(i)T} & \mathbf{r}_{,y}^{(i)T} & \mathbf{r}_{,z}^{(i)T} \end{bmatrix}^T, \quad (2)$$

where the following notations for gradients are used:

$$\mathbf{r}_{,\alpha}^{(i)} = \begin{bmatrix} r_{1,\alpha}^{(i)} \\ r_{2,\alpha}^{(i)} \\ r_{3,\alpha}^{(i)} \end{bmatrix} = \frac{\partial \mathbf{r}^{(i)}}{\partial \alpha}; \quad \alpha = x, y, z.$$

The interpolation functions for position can be obtained using the following set of basis polynomials

$$[1, x, y, z, xz, yz, yx, x^2, y^2, x^3, y^3, x^2y, y^2x, xyz, x^3y, xy^3]. \quad (3)$$

Note that the basis polynomials in Eq. (3) are incomplete, and for this reason, the element has linear terms only in transverse coordinate z . Accordingly, the displacement distribution is linear in the element's transverse direction. The interpolation for position is cubic in the in-plane coordinates x and y . The shape functions can be presented through use

of local normalized coordinates, such as $\xi, \eta, \zeta \in [-1 \dots 1]$, and are listed below:

$$\begin{aligned}
S_1 &= \frac{1}{8}(-1 + \xi)(1 - \eta)(\xi^2 + \xi + \eta^2 + \eta - 2), & S_2 &= \frac{1}{16}l_x(1 - \eta)(1 + \xi)(-1 + \xi)^2, \\
S_3 &= \frac{1}{16}l_y(1 - \xi)(\eta + 1)(-1 + \eta)^2, & S_4 &= \frac{1}{8}l_z\zeta(-1 + \xi)(-1 + \eta), \\
S_5 &= \frac{1}{8}(1 + \xi)(-1 + \eta)(\xi^2 - \xi + \eta^2 + \eta - 2), & S_6 &= \frac{1}{16}l_x(1 - \xi)(-1 + \eta)(1 + \xi)^2, \\
S_7 &= \frac{1}{16}l_y(1 + \xi)(\eta + 1)(-1 + \eta)^2, & S_8 &= \frac{1}{8}l_z\zeta(1 + \xi)(1 - \eta), \\
S_9 &= \frac{1}{8}(1 + \xi)(-\eta - 1)(\xi^2 - \xi + \eta^2 - \eta - 2), & S_{10} &= \frac{1}{16}l_x(-1 + \xi)(\eta + 1)(1 + \xi)^2, \\
S_{11} &= \frac{1}{16}l_y(1 + \xi)(-1 + \eta)(\eta + 1)^2, & S_{12} &= \frac{1}{8}l_z\zeta(1 + \xi)(\eta + 1), \\
S_{13} &= \frac{1}{8}(-1 + \xi)(\eta + 1)(\xi^2 + \xi + \eta^2 - \eta - 2), & S_{14} &= \frac{1}{16}l_x(1 + \xi)(\eta + 1)(-1 + \xi)^2, \\
S_{15} &= \frac{1}{16}l_y(-1 + \xi)(1 - \eta)(\eta + 1)^2, & S_{16} &= \frac{1}{8}l_z\zeta(\eta + 1)(1 - \xi)
\end{aligned} \tag{4}$$

where relations $\xi = 2x/l_x$, $\eta = 2y/l_y$ and $\zeta = 2z/l_z$ when the physical coordinate system x, y, z is placed along the middle of the element. These shape-functions can be represented in matrix form as:

$$\mathbf{S}_m = [S_1\mathbf{I} \quad S_2\mathbf{I} \quad S_3\mathbf{I} \quad \dots \quad S_{16}\mathbf{I},] \tag{5}$$

where \mathbf{I} is a 3×3 identity matrix. Due to the isoparametric property of the element, the kinematics can also be expressed in terms of local normalized coordinates $\mathbf{r} = \mathbf{S}_m(\xi, \eta, \zeta)\mathbf{e}$. The plate element with linearized transverse shear deformations is based on the same in-plane interpolation functions as the original fully parameterized plate element [9] but a slightly different approach for the interpolation of shear deformation is employed. To guarantee that parasitic strain distribution is zero, the nodal values are used instead of sampling points in [19].

Equations of motion for the element

The variational form of the equations of motion in the Lagrangian (material) description can be derived from the functional \mathcal{I} , see for example [20], which can be written as

$$\mathcal{I} = \int_{t_1}^{t_2} (W_{kin} - W_{pot}) dt, \tag{6}$$

where t_1 and t_2 are integration limits with respect to time t , W_{kin} is the kinetic energy of the element and W_{pot} is the potential energy which includes the internal strain energy W_{int} and the potential energy W_{ext} due to conservative external forces. The potential energy can be written as follows:

$$W_{pot} = W_{int} - W_{ext}. \tag{7}$$

In this study, non-conservative forces are not taken into account. The variation of the functional leads to

$$\delta\mathcal{I} = \delta \int_{t_1}^{t_2} (W_{kin} - W_{int} + W_{ext}) dt = 0. \tag{8}$$

The variations of the energies can be written as

$$\delta W_{kin} = \int_V \rho \dot{\mathbf{r}} \cdot \delta \dot{\mathbf{r}} dV, \tag{9}$$

$$\delta W_{int} = \int_V \mathbf{S} : \delta \mathbf{E} dV, \tag{10}$$

$$\delta W_{ext} = \int_V \mathbf{b} \cdot \delta \mathbf{r} dV, \tag{11}$$

where \cdot denotes the double dot product, ρ is the mass density, \mathbf{S} is the second Piola-Kirchhoff stress tensor, \mathbf{E} is the Green strain tensor and \mathbf{b} is the vector of body forces. In the special case of gravity, the body forces can be written as $\mathbf{b} = \rho \mathbf{g}$, where \mathbf{g} is the field of gravity. The Green strain tensor can be written as

$$\mathbf{E} = \frac{1}{2}(\mathbf{F}^T \mathbf{F} - \mathbf{I}), \quad (12)$$

where \mathbf{I} is the identity tensor and \mathbf{F} is the deformation gradient tensor, which can be presented in terms of the initial and current configurations $\bar{\mathbf{r}}$ and \mathbf{r} as follows:

$$\mathbf{F} = \frac{\partial \mathbf{r}}{\partial \bar{\mathbf{r}}} = \frac{\partial \mathbf{r}}{\partial \mathbf{x}} \left(\frac{\partial \bar{\mathbf{r}}}{\partial \mathbf{x}} \right)^{-1}. \quad (13)$$

Integrating the variation of the kinetic energy in Equation (6) by parts within the time interval t_1 and t_2 yields

$$\int_{t_1}^{t_2} \int_V \rho \dot{\mathbf{r}} \cdot \delta \mathbf{r} \, dV + \int_{t_1}^{t_2} \left(- \int_V \rho \ddot{\mathbf{r}} \cdot \delta \mathbf{r} \, dV - \int_V \mathbf{S} : \delta \mathbf{E} \, dV + \int_V \mathbf{b} \cdot \delta \mathbf{r} \, dV \right) dt = 0, \quad (14)$$

where the boundary condition term vanishes because the position vector is specified at the endpoints t_1 and t_2 . The weak form of the equations of motion for an element can be written as follows:

$$\int_V \rho \ddot{\mathbf{r}} \cdot \delta \mathbf{r} \, dV + \int_V \mathbf{S} : \delta \mathbf{E} \, dV - \int_V \mathbf{b} \cdot \delta \mathbf{r} \, dV = 0. \quad (15)$$

Using interpolation for the position vector \mathbf{r} , the variations of energy with respect to the nodal coordinates can be expressed. The variation of the kinetic energy can be represented as

$$\delta W_{kin} = \int_V \rho \ddot{\mathbf{r}} \cdot \delta \mathbf{r} \, dV = \ddot{\mathbf{e}}^T \int_V \rho \mathbf{S}_m^T \mathbf{S}_m \, dV \cdot \delta \mathbf{e}, \quad (16)$$

from which the mass matrix of the element can be identified as follows:

$$\mathbf{M} = \int_V \rho \mathbf{S}_m^T \mathbf{S}_m \, dV. \quad (17)$$

As can be concluded from Equation (17), the mass matrix is constant as it is not a function of the nodal coordinates. This will save time on computation, especially when an explicit time integration method is needed. However, this advantage may be marginal when the tangential stiffness matrix is needed which is the case in implicit time integration procedures. The virtual work for the externally applied forces can be written as

$$\delta W_{ext} = \int_V \mathbf{b}^T \delta \mathbf{r} \, dV = \int_V \mathbf{b}^T \mathbf{S}_m \, dV \cdot \delta \mathbf{e}, \quad (18)$$

where \mathbf{b} is the vector of body forces. The vector of externally applied forces can be identified from Equation (18) as follows:

$$\mathbf{F}_{ext} = \int_V \mathbf{b}^T \mathbf{S}_m \, dV. \quad (19)$$

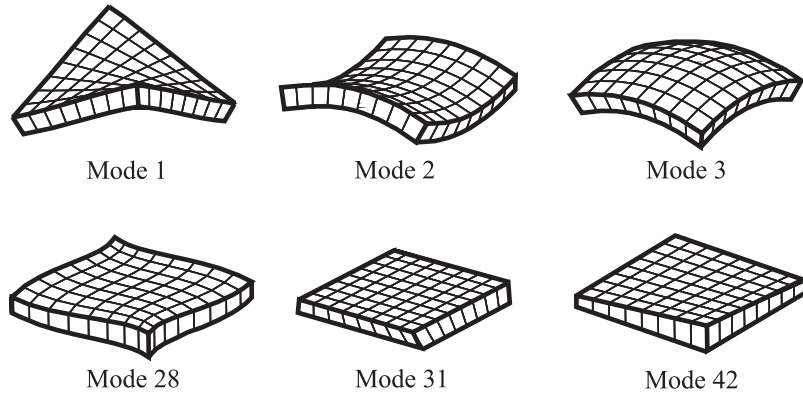


Figure 2. Some eigenmodes of a one fully-parametrized plate element.

The variation of the strain energy with respect to the nodal coordinates can be written as

$$\delta W_{int} = \int_V \mathbf{S} : \delta \mathbf{E} dV = \int_V \mathbf{S} : \frac{\partial \mathbf{E}}{\partial \mathbf{e}} dV \cdot \delta \mathbf{e}, \quad (20)$$

The vector of elastic forces can be identified from Equation (20) as follows:

$$\mathbf{F}_e = \int_V \mathbf{S} : \frac{\partial \mathbf{E}}{\partial \mathbf{e}} dV. \quad (21)$$

The equations of motion can be present in explicit form as follows

$$\mathbf{M} \ddot{\mathbf{e}} + \mathbf{F}_e(\mathbf{e}) = \mathbf{F}_{ext}, \quad (22)$$

where \mathbf{e} can be solved by using explicit or implicit integrator. In case of Newton's iteration, the tangential stiffness matrix is often found by using finite differences.

Numerical examples

In this section, static and linearized dynamic problems are solved to demonstrate possible problems in the fully-parametrized plate elements. In order to emphasize the capacity of fully-parametrized plate element, eigenmodes for one element are presented in Figure 2. Special feature in the fully-parametrized plate elements are in-plane modes, see for example modes 28, 31 and 42 in Figure 2, where modes 31 and 42 are clearly shear and thickness modes. As can be seen, first lowest modes are similar to the thin plate theory, see for example [21, 22]. The convergence of the first mode (see top left mode in Figure 2 is considered, in which the relative plate thickness is assumed to be $H/L = 0.001$.

As can be seen from the Figure 3, the convergence of the first mode of ANCF-P48lsa is considerably faster than in the case of ANCF-P48. Furthermore, figure 3 shows that ANCF-P48lsa is not sensitive in terms of the convergence of the first mode of the thin plate. Accordingly, in the case of a thin plate, the convergence of the first mode does not depend on a relative plate thickness of H/L , as such is the case for ANCF-P48. This type of locking phenomenon is known as shear locking. However, it is shown in [22] that under pure bending, the plate elements do not show any locking phenomena.

It shall be noted that fully-parametrized plate element does not suffer from Poisson locking because it includes the trapezoidal deformation mode of the cross-section. Although, it still suffers from thickness locking which is a problem when three-dimensional

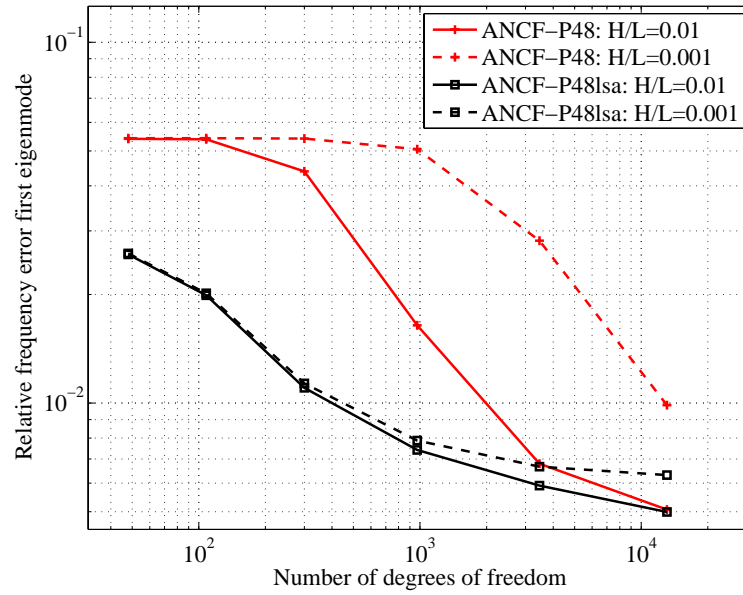


Figure 3. Convergences of the first mode normalized by analytical solution for free (ffff) square plate as calculated by the ANCF-P48 and ANCF-P48lsa with Poisson factor $\nu=0.3$. Two different relative plate thickness of $H/L=0.01$ and $H/L=0.001$ were used.

elasticity is used. Therefore, in order to show the effect of shear and thickness locking, a simple static problem is considered. In this example, a plate is constrained with a simply supported condition and is loaded by the normal uniform force in the transverse direction as shown in Fig. 4.

The parameters used in the plate example are as follows: length $L = 1$ m, Young's modulus $E = 210 \cdot 10^9 \text{ N/m}^2$, shear modulus $G = E/2(1 + \nu)$, shear correction factor $k_s = 1$, Poisson's ratio $\nu = 0.3$ and the uniformly distributed load is expressed as $q = -5 \cdot 10^6 H^3 \text{ N/m}^3$. The computed displacements for elements ANCF-P48 and ANCF-P48lsa are normalized by the analytical solution. This example is also used in [22], where analytical solutions based on the Reissner-Mindlin theory are presented. In the case of a finite element solution, a uniformly distributed load is defined as a consistent load vector

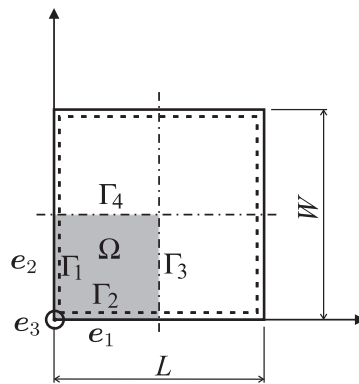


Figure 4. Simply supported plate, its sub domain Ω and the coordinate system.

as follows:

$$F_{ext} = \int_V \mathbf{b}^T \mathbf{S} dV \quad (23)$$

where the body force is $\mathbf{b} = [0, q/H, 0]^T$. In order to minimize the number of degrees of freedom, double symmetry for the plate under constant loading is used. In double symmetry, the boundary conditions of sub domain are Ω boundary Γ_3 are as: $r_1 = 0$, $r_{3,x} = 0$ and $r_{1,z} = 0$ and for boundary as Γ_4 : $r_2 = 0$, $r_{2,z} = 0$ and $r_{3,y} = 0$. The boundaries Γ_1 and Γ_2 are simply supported, therefore r_1 and r_2 are fixed for boundary Γ_1 and r_2 and r_3 for Γ_2 . The deflection at the middle of the plate in Table 1 is normalized by the analytical result. In Table, results of the plate element with plane stress assumption, denoted by ANCF-P48ps, are presented.

Table 1. Normalized transverse displacement at center of the plate loaded by a uniform loading. A relative plate thickness of $H/L = 0.01$ was used.

Mesh	ANCF-P48 ($\nu = 0.3$)	ANCF-P48lsa ($\nu = 0.3$)	ANCF-P48 ($\nu = 0$)	ANCF-P48lsa ($\nu = 0$)	ANCF-P48ps ($\nu = 0.3$)
2x2	0.02388	0.6669	0.01879	0.8702	0.02411
4x4	0.3134	0.7465	0.3015	0.9841	0.3428
8x8	0.6868	0.7463	0.8860	0.9994	0.8304
16x16	0.7377	0.7447	0.9908	1.002	0.9030
32x32	0.7435	0.7447	1.002	1.003	0.9110
64x64	0.7454	0.7456	1.006	1.006	0.9137
128x128	0.7467	0.7468	1.009	1.009	0.9157

It can be seen from results in Table 1 that using the special case $\nu=0$ in three-dimensional elasticity, thickness locking can be avoided. Therefore, both plate elements converge to the analytic solution in thin plate cases since coupling between bending and shear deformation is neglected. To account for three-dimensional elasticity in the plate and shell formulations without thickness locking when $\nu \neq 0$, the transverse normal strain has to be interpolated at least linearly over the thickness direction [23]. The ANCF-P48ps shows that the inaccurate solution is not only due to low order interpolation for transverse deformations but, in part, due to in-plane shear deformations. Also results of cantilever plate analyzed by ANCF-P48ps [22] support to this claim because cantilever plate with correct boundary conditions does not include in-plane shear deformations and therefore, the solution corresponded with analytical solution. In case of ANCF plate elements, the transverse normal strain is interpolated by using constant distribution in the thickness direction.

Conclusions

In this study, the fully-parametrized ANCF plate element is described. An original fully-parametrized plate element suffers from different locking phenomena and therefore, the numerical example is solved by using fully-parametrized plate element where shear locking is avoided similarity to the MITCH-plate elements. It can be concluded that the fully-parameterized ANCF plate elements are promising elements due to the possibility for the usage of three-dimensional elasticity. However, the formulation still suffers from lockings, mainly due to the assumptions for kinematics, such as the assumption according

to which the fiber remains straight during deformation. The main problem in these fully-parametrized ANCF plate elements is the thickness locking which is typical problem in continuum plate elements where three-dimensional elasticity is adopted. Therefore, both introduced plate elements based on the absolute nodal coordinate formulation converged to the same incorrect solution in used numerical examples. In future work, in order to use known material models from general continuum mechanics, the thickness locking have to overcome in case of fully-parametrized plate elements. Furthermore, there is a number of interesting research topics where ANCF plate elements may be useful. For example, the derivation of composite ANCF plate is still not shown. In addition, in order to clarify the efficiency of ANCF plate elements, the comparison study to the other continuum plate element is needed.

References

- [1] S. Ahmad, B. M. Irons and O. C. Zienkiewich. Analysis of thick and thin shell structures by curved finite elements. *International Journal for Numerical Methods in Engineering*, 2(3):419–451,1970.
- [2] E.N. Dvorkin, K-J. Bathe. A continuum mechanics based four-node shell element for general nonlinear analysis. *Engineering Computations*, 77(1):77–88, 1984.
- [3] A. Avello, J. García de Jalón and E. Bayo. Dynamic analysis of flexible multibody systems using cartesian co-ordinates and large displacement theory. *International Journal for Numerical Methods in Engineering*, 32(8):1543–1563, 1991.
- [4] J. Rhim. *A vectorial approach to finite rotation beams*. PhD thesis, University of Maryland, 1996.
- [5] T. Belytschko, W. K. Liu and B. Moran. Nonlinear Finite Elements for Continua and Structures. *Nonlinear Finite Elements for Continua and Structures*. Wiley, Chichester, 2000. Repr. 2001.
- [6] A. A. Shabana. Flexible multibody dynamics: Review of past and recent developments. *Multibody System Dynamics*, 1(2):189–222, 1997.
- [7] M. A. Omar and A. A. Shabana. A two-dimensional shear deformable beam for large rotation and deformation problems. *Journal of Sound and Vibration*, 243(3):565–576, 2001.
- [8] A. A. Shabana and Y. R. Yakoub. Three dimensional absolute nodal coordinate formulation for beam elements: theory. *Journal of Mechanical Design*, 123(4):606–613, 2001.
- [9] A. M. Mikkola and A. A. Shabana. A non-incremental finite element procedure for the analysis of large deformations of plates and shells in mechanical system applications. *Multibody System Dynamics*, 9(3):283–309, 2003.
- [10] O. N. Dmitrochenko and D. YU. Pogorelov. Generalization of plate finite elements for absolute nodal coordinate formulation. *Multibody System Dynamics*, 10(1):17–43, 2003.
- [11] A. L. Schwab and J. P. Meijaard. Comparison of three-dimensional flexible beam elements for dynamic analysis: Finite element method and absolute nodal coordinate formulation. *Proceedings of the IDEC/CIE 2005, ASME 2005 International Design Engineering Technical Conferences, Paper Number DETC2005-85104*, Long Beach, USA, 24 - 28 September 2005.

- [12] J. Gerstmayr and A. A. Shabana. Analysis of thin beams and cables using the absolute nodal co-ordinate formulation. *Nonlinear Dynamics*, 45(1–2):109–130, 2006.
- [13] S. von Dombrowski. Analysis of Large Flexible Body Deformation in Multibody Systems Using Absolute Coordinates. *Multibody System Dynamics*, 8(4):409–432, 2002.
- [14] H. Sugiyama and A. A. Shabana. On the Use of Implicit Integration Methods and the Absolute Nodal Coordinate Formulation in the Analysis of Elasto-Plastic Deformation Problems. *Nonlinear Dynamics*, 37(3):245–270, 2004.
- [15] A. A. Shabana and A. P. Christensen. Three-dimensional absolute nodal co-ordinate formulation: plate problem. *International journal for numerical methods in engineering*, 40(15):2775–2790, 1997.
- [16] O. Dmitrochenko and A. Mikkola. Two simple triangular plate elements based on the absolute nodal coordinate formulation. *Journal of Computational and Nonlinear Dynamics*, 3(041012):1–8, 2008.
- [17] K. Dufva and A. A. Shabana. Analysis of Thin Plate Structures Using the Absolute Nodal Coordinate Formulation. *Journal of Multi-body Dynamics*, 219(4):345–355, 2006.
- [18] A. M. Mikkola and M. K. Matikainen. Development of elastic forces for a large deformation plate element based on the absolute nodal coordinate formulation. *Journal of Computational and Nonlinear Dynamics*, 1(2), 103–108, 2006.
- [19] M. Bischoff and E. Ramm. Shear deformable shell elements for large strains and rotations. *International Journal for Numerical Methods in Engineering*, 40(23):4427–4449, 1997.
- [20] H. Goldstein. *Classical mechanics*. Addison-Wesley, Reading (MA), Second edition, 1980.
- [21] A. L. Schwab, J. Gerstmayr and J. P. Meijaard. Comparison of Three-Dimensional Flexible Thin Plate Elements for Multibody Dynamic Analysis: Finite Element Formulation and Absolute Nodal Coordinate Formulation. Proceedings of the ASME 2007 Int. Design engineering technical conferences & Computers and information in engineering conference, Las Vegas, USA, 4–7 September 2007.
- [22] M. K. Matikainen and A. L. Schwab and A. Mikkola. Comparison of Two Moderately Thick Plate Elements Based on the Absolute Nodal Coordinate Formulation. Multibody Dynamics 2009, ECCOMAS Thematic Conference, Warsaw, Poland, 29 June - 2 July 2009.
- [23] E. Carrera, S. Brischetto. Analysis of thickness locking in classical, refined and mixed multilayered plate theories. *Composite Structures*, 82(4):549–562, 2008.

Marko K. Matikainen, Aki M. Mikkola
 Department of Mechanical Engineering
 Lappeenranta University of Technology
 Skinnarilankatu 34, FI-53850 Lappeenranta, Finland
 e-mail: marko.matikainen@lut.fi, aki.mikkola@lut.fi

A. L. Schwab
 Laboratory of Engineering Mechanics
 Delft University of Technology
 Megelweg 2, NL 2628 CD Delft, The Netherlands
 e-mail: a.l.schwab@tudelft.nl